

# Predictive Power of Clean Bed Filtration Theory for Fecal Indicator Bacteria Removal in Stormwater Biofilters

Emily A. Parker,<sup>†</sup> Megan A. Rippey,<sup>†</sup> Andrew S. Mehring,<sup>‡</sup> Brandon K. Winfrey,<sup>§</sup> Richard F. Ambrose,<sup>§</sup> Lisa A. Levin,<sup>||</sup> and Stanley B. Grant<sup>†\*</sup>

<sup>†</sup>Department of Civil and Environmental Engineering, Henry Samueli School of Engineering, University of California, Irvine, California 92697, United States

<sup>‡</sup>Scripps Institution of Oceanography, University of California, San Diego, California 92093, United States

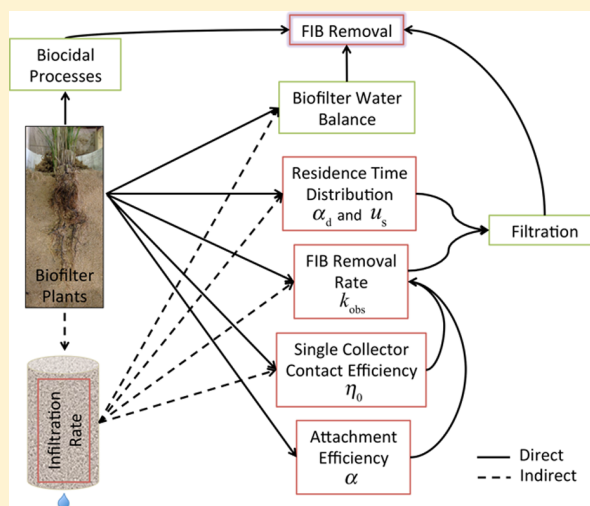
<sup>§</sup>Department of Environmental Health Sciences, Jonathan and Karen Fielding School of Public Health, University of California, Los Angeles, California 90095, United States

<sup>||</sup>Center for Marine Biodiversity and Conservation, Scripps Institution of Oceanography, University of California, San Diego, California 92093-0218, United States

<sup>†</sup>Department of Chemical Engineering and Materials Science, Henry Samueli School of Engineering, University of California, Irvine, California 92697, United States

## Supporting Information

**ABSTRACT:** Green infrastructure (also referred to as low impact development, or LID) has the potential to transform urban stormwater runoff from an environmental threat to a valuable water resource. In this paper we focus on the removal of fecal indicator bacteria (FIB, a pollutant responsible for runoff-associated inland and coastal beach closures) in stormwater biofilters (a common type of green infrastructure). Drawing on a combination of previously published and new laboratory studies of FIB removal in biofilters, we find that 66% of the variance in FIB removal rates can be explained by clean bed filtration theory (CBFT, 31%), antecedent dry period (14%), study effect (8%), biofilter age (7%), and the presence or absence of shrubs (6%). Our analysis suggests that, with the exception of shrubs, plants affect FIB removal indirectly by changing the infiltration rate, not directly by changing the FIB removal mechanisms or altering filtration rates in ways not already accounted for by CBFT. The analysis presented here represents a significant step forward in our understanding of how physicochemical theories (such as CBFT) can be melded with hydrology, engineering design, and ecology to improve the water quality benefits of green infrastructure.



## INTRODUCTION

Urban runoff poses both challenges and opportunities. Hydrological alterations associated with urbanization universally increase the volume of runoff and pollutant loads delivered to streams, lakes, and the coastal ocean during storms.<sup>1–4</sup> On the other hand, urban runoff can be transformed into a valuable water resource through the adoption of green infrastructure, also known as low impact development (LID). LID technologies capture and treat urban runoff before it reaches sensitive receiving waters.<sup>5–7</sup> The treated water can be used to support local groundwater supplies (if infiltrated) and as a source of nonpotable water for irrigation and toilet flushing (if harvested).<sup>7–11</sup>

Biofilters (also known as rain gardens or bioretention systems) are a particularly versatile LID technology. They are vertically oriented filtration systems in which runoff ponds at the top and

percolates by gravity through planted and variably saturated filter media.<sup>12,13</sup> Because they have relatively small areal footprints (e.g., compared to constructed wetlands), biofilters can be integrated into the urban landscape over a range of scales.<sup>14</sup> They can also be engineered to achieve prespecified levels of runoff harvesting and infiltration, for example with the goal of maintaining and/or restoring preurban flow regimes in streams.<sup>7,15</sup>

Among their water quality benefits, biofilters may be useful for removing fecal indicator bacteria (FIB) from dry and wet weather urban runoff.<sup>16–22</sup> FIB, which include *Escherichia coli* and

Received: February 10, 2017

Revised: April 18, 2017

Accepted: April 26, 2017

Published: April 26, 2017

enterococci bacteria, are routinely used by public health officials to assess the human health risk of recreating in fresh and marine surface waters.<sup>23,24</sup> FIB are often present at high concentrations in urban runoff,<sup>25–28</sup> and consequently thousands of runoff-impacted inland and coastal beaches in the U.S. are periodically closed to the public because FIB concentrations exceed state or federal limits.<sup>29</sup> The cost of these water quality impairments—measured in recreational waterborne illness,<sup>30</sup> lost recreational opportunity,<sup>31</sup> and cleanup<sup>32</sup>—is staggering. For example, deployment of LID and education programs to reduce stormwater runoff-associated FIB pollution at recreational beaches in San Diego (California) could cost the city up to \$3.7 billion (2011 U.S. dollars).<sup>32</sup> For all of these reasons, there is an urgent need to understand how engineering design influences FIB removal in green infrastructure, in general, and biofilters, in particular.<sup>33,34</sup>

Clean bed filtration theory (CBFT) may be helpful in this regard, as it is routinely used to design packed bed filtration systems for the removal of colloidal particles in water.<sup>35,36</sup> CBFT predicts particle removal by physicochemical filtration, which involves two steps: (1) transport of particles to the surface of grains within a packed bed filter (described by a dimensionless “single collector contact efficiency”), and (2) attachment of particles to the grain surface (described by a dimensionless “attachment efficiency”). While physicochemical filtration is often cited as an important mechanism for FIB removal in biofilters,<sup>19,34,37–40</sup> the theory’s many underlying assumptions may limit its utility for predicting the filtration of microorganisms in biofilters.<sup>37,41,42</sup>

In this study we hypothesize that CBFT is a useful predictor of FIB removal in biofilters, but only when considered in the context of the many other factors that can affect treatment performance, such as the presence and type of upright vegetation in these systems, presence of a submerged zone, antecedent dry period (ADP), and biofilter age. To test this hypothesis we: (1) estimate observed first-order removal rates from new and previously published FIB challenge experiments that collectively capture a wide range of infiltration rates, degrees of saturation, ADPs, plant types, and study designs; (2) use CBFT to predict theoretical first-order removal rates for these experiments, ignoring the nonideal conditions that might preclude a direct application of the theory; and (3) use multiple linear regression to determine the fraction of the observed variance in FIB removal rates that can be attributed to CBFT versus other potentially important hydrological, engineering design, and ecological features.

## METHODS

**Chandrasena et al. (2014) Experiment.** Chandrasena et al.<sup>16</sup> (hereafter referred to as “CH”) conducted a series of FIB removal experiments in laboratory biofilter columns (0.6 m deep, 0.15 m diameter). These were constructed with a layer of loamy sand at the top (0.3 m thick), a transition layer of washed coarse sand with 5% (v/v) finely shredded sugar cane mulch and 5% (v/v) pinewood chips without bark (0.2 m thick), and a gravel drainage layer at the bottom (0.1 m thick). This configuration is typical of biofilters in Australia. The transition layer is included to prevent the filter media from washing into the gravel layer, while the gravel layer is included to convey the treated water to drain pipes if the biofilter is lined, or shallow groundwater if the biofilter is unlined.<sup>12</sup> These previously published FIB challenge experiments were conducted by administering a single dose (either 3.7 or 4.2 L, representing the different climatic conditions

in the Australian cities of Melbourne and Perth, respectively) of synthetic stormwater, spiked with a pure culture of *E. coli* (ATCC #11775), to partially saturated biofilters. The synthetic stormwater consisted of dechlorinated tap water, sediment (passed through a 300- $\mu$ m sieve) from a nearby stormwater wetland, and reagent grade salts and heavy metals in final concentrations consistent with the chemical makeup of urban stormwater runoff in Melbourne.<sup>43</sup> *E. coli* concentrations (in units of most probable number (MPN) per 100 mL of sample) were quantified using the culture-based defined substrate technology IDEXX Colilert, implemented in a 96-well Quanti-Tray format (IDEXX, Westbrook, ME). The biofilter columns ( $n = 90$ ) were placed in a purpose-built greenhouse facility on the Monash University campus in Melbourne that allowed for realistic (i.e., outdoor) light and temperature variability, but prevented rain from falling on the columns, allowing the authors to control the volumes and quality of water entering the columns. Of the 90 columns, 20 were not planted (i.e., unplanted controls) while the other 70 were planted with a single species of upright vegetation. The palette of vegetation species included common biofilter plants spanning three different plant growth forms: two shrubs, one forb, and four graminoid species (consisting of one sedge, two grasses, and one lawn grass). The FIB challenge experiments consisted of seven dosing events conducted over the course of eight months, and therefore the age of the biofilters varied from approximately 8 to 16 months. Prior to the FIB challenge experiments, all columns (both vegetated and unplanted controls) were periodically watered with synthetic stormwater (defined above) with an ADP varying from 0 to 14 days, a typical range for the Melbourne area.<sup>44</sup> Here we focus on a subset of CH’s FIB challenge experiments ( $n = 196$ ) for which the reported infiltration rate was greater than  $7.0 \times 10^{-6} \text{ m s}^{-1}$ ; this threshold represents the lower bound of infiltration rates for which our CBFT correlations apply (see later), and is at the low end of recommended hydraulic conductivities for biofilters in temperate and tropical environments.<sup>45</sup>

**2015/2016 Follow-Up Experiment.** CH’s challenge experiments were designed to evaluate FIB removal under a realistic range of field operating conditions. As a result, application of CBFT to these data is complicated by the fact that the columns were partially saturated and subject to transient flow during dosing events. We therefore carried out additional FIB challenge experiments to evaluate CBFT under more idealized (but less realistic) operating conditions. Six laboratory columns (0.8 m deep, 0.24 m diameter) were constructed in the Hydraulics Laboratory at Monash University (Melbourne, Australia) using the same filter media as CH, but arranged in slightly thicker layers; namely, loamy sand (0.4 m) overlying a transition layer (0.3 m) overlying gravel (0.1 m). Three of the biofilters were planted with the sedge (graminoid) *Carex appressa* and three were unplanted (unplanted controls). The columns were illuminated with grow lights (12 h on, 12 h off) and watered twice per week with the same synthetic stormwater described earlier. Two sets of FIB dosing experiments were conducted, one when the biofilters were approximately 1 month old (July 2015) and another when they were approximately 9 months old (March 2016). While our biofilters were constructed based on the design described in CH, our FIB challenge experiments differed in six significant aspects: (1) source of FIB (a pure culture of *E. coli* spiked into synthetic stormwater in CH, secondary treated sewage from the Melbourne Eastern Treatment Plant in our experiments); (2) degree of saturation (biofilters were partially saturated in CH, biofilters were fully

saturated in our experiment); (3) flow conditions (the pulse of FIB was applied to the biofilter as a single dose of spiked stormwater in CH, tap water was continuously flowing through our biofilters when the pulse of secondary-treated sewage was applied in our experiment, see [Supporting Information, SI, Section S1](#) for details); (4) method used to assess FIB removal (measurements of the FIB concentration in a single composite sample of the biofilter effluent collected over approximately 24 h in CH, time-resolved measurements of FIB breakthrough curves in our experiment); (5) the FIB groups measured (*E. coli* in CH, *E. coli* and enterococci bacteria in our experiment); and (6) the range of infiltration rates interrogated ( $I = 8 \times 10^{-6}$  to  $7.0 \times 10^{-5}$  m s<sup>-1</sup> in CH,  $I = 1 \times 10^{-4}$  to  $2 \times 10^{-4}$  m s<sup>-1</sup> in our experiments). FIB concentrations (in units of MPN per 100 mL of sample) were quantified using IDEXX Colilert (*E. coli*) and Enterolert (enterococci bacteria) implemented in a 96-well Quanti-Tray format (IDEXX, Westbrook, ME). Secondary-treated sewage is a reasonable (although imperfect) proxy for urban runoff. The concentration of *E. coli* and enterococci bacteria in the secondary-treated sewage (about  $2 \times 10^4$  to  $2.5 \times 10^4$  MPN 100 mL<sup>-1</sup> for *E. coli* and about  $3 \times 10^3$  to  $7 \times 10^3$  MPN 100 mL<sup>-1</sup> for enterococci bacteria) are within the range reported previously for stormwater runoff ( $110$  to  $2 \times 10^6$  MPN 100 mL<sup>-1</sup> for *E. coli* (median  $9 \times 10^3$  MPN 100 mL<sup>-1</sup>) and  $<1$  to  $8 \times 10^5$  MPN 100 mL<sup>-1</sup> for enterococci bacteria (median  $5 \times 10^3$  MPN 100 mL<sup>-1</sup>)).<sup>26</sup> However, the conductivity of the secondary-treated sewage ( $900 \mu\text{S cm}^{-1}$ ) is high for stormwater runoff (event mean concentrations ranging from  $211$  to  $730 \mu\text{S cm}^{-1}$ , maximum  $1992 \mu\text{S cm}^{-1}$ ).<sup>46</sup>

**Salt Pulse Experiment for Estimating Residence Time Distributions.** In general, the treatment performance of packed bed filters depends on the rate at which contaminants are removed within the filter (e.g., by physicochemical filtration) and the residence time distribution of water passing through the filter.<sup>47</sup> To model the residence time distribution we adopted the dispersed plug flow model, which requires estimates for the interstitial velocity  $u_s$  (m s<sup>-1</sup>) and dispersivity  $\alpha_d$  (m); the former is a measure of how quickly water and mass are transported through the pore spaces of the filter by advection, while the latter represents longitudinal mixing within the filter by mechanical dispersion. The interstitial velocity can be represented as the ratio of the infiltration rate (or Darcy flux) ( $I$ , m s<sup>-1</sup>) and the average porosity of the filter bed ( $\theta$ , unitless):  $u_s = I/\theta$ . To estimate these parameters we carried out a salt pulse experiment on the same set of biofilter columns used in the 2015/2016 experiment (described above) under saturated and constant flow conditions. Two different conservative tracers were used, NaCl (in July 2015) and NaBr (in March 2016) (see [SI, Section S1](#) for details). Water samples ( $\sim 80$  per biofilter) were collected from the biofilter outlet at a variable sampling frequency (ranging from  $0.067$  to  $1 \text{ min}^{-1}$ ) for approximately 4 h following the addition of the salt pulse. The samples were then analyzed for conductivity (NaCl, July 2015) and bromide concentration (NaBr, March 2016) using a hand-held conductivity probe (model HQ40d, Hach, Loveland, CO) and an Orion bromide electrode (ThermoFisher Scientific, Waltham, MA); calibration curves were prepared immediately prior to each experiment. Values for  $\alpha_d$  and  $u_s$  (and by inference  $\theta$ ) were then estimated by fitting the observed tracer breakthrough curves to the dispersed plug flow model:<sup>47</sup>

$$C_{\text{exit}}^{\text{salt}}(\tau) = \frac{M_0^{\text{salt}}}{IA} \sqrt{\frac{u_s}{4\pi\tau\alpha_d}} \exp\left[-\frac{(L - u_s\tau)^2}{4\alpha_d u_s\tau}\right] \quad (1)$$

In this equation,  $C_{\text{exit}}^{\text{salt}}(\tau)$  (g L<sup>-1</sup>) represents the breakthrough concentration of salt at an elapsed time  $\tau$  since the addition of the pulse,  $M_0^{\text{salt}}$  (g) represents the mass of salt added to the biofilter,  $L$  (m) is the biofilter depth,  $A$  (m) is the biofilter cross-sectional area, and all other variables have been previously defined. For the fitting step, we adopted Bayesian inference using Monte Carlo Markov chain simulation with the Differential Evolution Adaptive Metropolis (DREAM) algorithm.<sup>48,49</sup>

**Observed Filtration Rate Constants ( $k_{\text{obs}}$ ).** CBFT represents particle removal in a filter by a first-order rate constant ( $k_{\text{CBFT}}$ , s<sup>-1</sup>, calculated as described later). In this paper we compare the first-order removal rate constant predicted by CBFT,  $k_{\text{CBFT}}$ , with a first-order rate constant estimated from the FIB challenge experiment, referred to here as an “observed” first-order rate constant ( $k_{\text{obs}}$ , s<sup>-1</sup>). Estimating the latter parameter involved two steps: (1) for each FIB challenge experiment (both ours and CH’s) we estimated the mass of FIB removed by passage through the biofilter (i.e., the mass ratio  $M_{\text{exit}}^{\text{FIB}}/M_0^{\text{FIB}}$  where  $M_0^{\text{FIB}}$  and  $M_{\text{exit}}^{\text{FIB}}$  represent the mass of FIB, both in units of MPN, entering and exiting the biofilter column); and (2) for each mass ratio we calculated a corresponding first-order rate constant  $k_{\text{obs}}$  assuming that FIB undergo first-order removal and that the residence time distribution can be described by the dispersed plug flow model (see last section). These two steps are detailed next.

The mass ratios were calculated as follows. CH assessed FIB removal by taking the ratio of the FIB concentration in a composite sample of the biofilter effluent ( $C_{\text{exit}}^{\text{FIB}}$ , MPN 100 mL<sup>-1</sup>) and in the dose of spiked stormwater applied to the biofilter inlet ( $C_0^{\text{FIB}}$ , MPN 100 mL<sup>-1</sup>):  $C_{\text{exit}}^{\text{FIB}}/C_0^{\text{FIB}}$ . Provided that roughly equal volumes of stormwater enter and exit the column, the mass ratio can be calculated directly from their reported concentration ratio:  $M_{\text{exit}}^{\text{FIB}}/M_0^{\text{FIB}} \approx C_{\text{exit}}^{\text{FIB}}/C_0^{\text{FIB}}$ . CH added 3.7 or 4.2 L of spiked stormwater to the column (depending on the climate being simulated), and reported that the volume of water drained from the biofilters declined with increasing ADP (average of 3.4 L after a three-day dry period versus 2.6 L after a two-week dry period); data on the water added and drained from each column were not reported. By equating the mass and concentration ratios, we may over- or underestimate the actual FIB mass removal in CH’s experiments (also note that water and FIB retained in one dosing event may be released in the next dosing event). For the 2015/2016 experiments, on the other hand, we calculated the initial FIB mass  $M_0^{\text{FIB}}$  from the product of the FIB concentration measured in the secondary-treated sewage and the volume of the sewage pulse added to the biofilter inlet. The mass of FIB exiting the biofilter  $M_{\text{exit}}^{\text{FIB}}$  was estimated by numerically integrating the measured FIB breakthrough curves, after subtracting out the background FIB concentration ( $20$  MPN 100 mL<sup>-1</sup> and  $2$  MPN 100 mL<sup>-1</sup> for *E. coli* and enterococci bacteria, respectively).

For each value of the mass ratio  $M_{\text{exit}}^{\text{FIB}}/M_0^{\text{FIB}}$  estimated by the above approach, [eq 2](#) (derivation in [ref 50](#)) was numerically solved to yield a corresponding first-order rate constant  $k_{\text{obs}}$  given known values for the infiltration rate ( $I$ ) and biofilter depth ( $L$ ), in addition to porosity ( $\theta$ ), and dispersivity ( $\alpha_d$ ) values estimated from the salt pulse experiment (see last section). We used column-specific porosities and dispersivities ([Table S1](#)) for analyzing the 2015/2016 experiments; however, this information was not available for the CH biofilters so we adopted values

averaged across the 2015/2016 experiments:  $\theta = 0.4$  (both planted and unplanted biofilters),  $\alpha_d = 0.04$  m (planted biofilters) and  $\alpha_d = 0.01$  m (unplanted biofilters).

$$\frac{M_{\text{exit}}^{\text{FIB}}}{M_0^{\text{FIB}}} = \frac{4a \exp\left(\frac{L}{2\alpha_d}\right)}{(1+a)^2 \exp\left(a\frac{L}{2\alpha_d}\right) - (1-a)^2 \exp\left(-a\frac{L}{2\alpha_d}\right)}$$

$$a = \sqrt{1 + 4\frac{k_{\text{obs}}\alpha_d\theta}{I}}$$
(2)

**Observed Single Collector Contact Efficiency.** One of the master variables in CBFT is the single collector contact efficiency  $\eta_0$  (unitless), defined as the rate at which particles strike a collector over the rate at which particles flow toward the collector.<sup>35</sup> Equation 3, obtained from mass balance over a differential slice of a filter<sup>36</sup> describes the relationship between the observed single collector contact efficiency  $\eta_{\text{obs}}$  (unitless) and the observed first-order rate constant  $k_{\text{obs}}$ . In this equation,  $d_c$  is the collector diameter (m),  $\alpha$  (unitless) is the attachment efficiency (fraction of FIB-grain collisions that result in attachment), and all other variables are defined previously.

$$\eta_{\text{obs}} = \frac{2}{3} \frac{k_{\text{obs}}d_c\theta}{\alpha(1-\theta)I}$$
(3)

Observed single collector contact efficiencies ( $\eta_{\text{obs}}$ ) were calculated for each FIB challenge experiment by setting  $\alpha = 1$  and substituting experimentally determined values for  $k_{\text{obs}}$ ,  $I$ ,  $\theta$  (see above); the collector diameter ( $d_c = 9.3 \times 10^{-4}$  m) was calculated from the median grain size of each filter media layer weighted by the corresponding thickness of each layer. The attachment efficiency was set to unity because, as noted in Tufenkji and Elimelech,<sup>51</sup> theories for estimating this parameter are currently inaccurate. By setting  $\alpha = 1$  in eq 3, our estimates for  $\eta_{\text{obs}}$  represent lower-limit values.

**Theoretical Single Collector Contact Efficiency.** Typically, three transport mechanisms are considered when predicting the theoretical single collector contact efficiency  $\eta_0$ : (1) particle collision with the collector by interception ( $\eta_I$ , particles moving along a streamline intercept collectors due to physical size); (2) gravitational sedimentation ( $\eta_G$ , particles with densities greater than water settle onto the collector surface); and (3) Brownian diffusion ( $\eta_D$ , Brownian motion of particles resulting in contact with a collector):<sup>51</sup>

$$\eta_0 = \eta_D + \eta_I + \eta_G$$
(4)

Tufenkji and Elimelech<sup>51</sup> developed a set of correlation equations for predicting  $\eta_D$ ,  $\eta_I$ , and  $\eta_G$  in saturated porous media, based on numerical simulations of the convective-diffusion equation for particle transport around a collector, accounting for both hydrodynamic interactions and van der Waals forces that develop between particle and collector on close approach.<sup>51</sup> We used these correlations and eq 4 to calculate theoretical values of  $\eta_0$  using parameter values appropriate for the biofilter experiments included in this study (see SI Section S2).

**Multiple Linear Regression.** To determine if CBFT is predictive of FIB removal in biofilters we used multiple linear regression (MLR) conducted in R software<sup>52</sup> to estimate the fraction of variance in the observed FIB removal rate ( $k_{\text{obs}}$ ) that is explained by the CBFT-predicted removal rate ( $k_{\text{CBFT}}$ , calculated as described below) as compared to other environmental and

biofilter design features. Two different MLR models were evaluated: (1) the Total Model which included data from both CH and the 2015/2016 experiments, and (2) the Partial Model which included data only from CH (2015/2016 experiments excluded). For the Partial Model we adopted the observed filtration rate ( $k_{\text{obs}}$ ) as the dependent variable, and the following predictor variables: (1)  $k_{\text{CBFT}}$  ( $\text{s}^{-1}$ ), (2) biofilter age (months), (3) ADP (days), (4) submerged zone presence or absence, and (5) a set of three binary dummy variables for plant type (e.g., shrub, graminoid, or forb). The same dependent and predictor variables were adopted for the Total Model, but a new binary predictor variable “Study” was added to account for possible effects of differences in the two studies. Theoretical filtration rate constants ( $k_{\text{CBFT}}$ ) were calculated from eq 5 based on Tufenkji and Elimelech’s theoretical correlations for the single collector contact efficiencies ( $\eta_0$ , see above and SI Section 2), known values of the infiltration rate ( $I$ ) and collector diameter ( $d_c$ ), and the average column porosities ( $\theta$ ) estimated from the salt pulse experiments:

$$k_{\text{CBFT}} = \frac{3}{2} \frac{(1-\theta)I}{d_c\theta} \eta_0$$
(5)

Equation 5 is obtained by rearranging eq 3, substituting  $k_{\text{CBFT}}$  for  $k_{\text{obs}}$ , and assuming the attachment efficiency is equal to unity. FIB die-off and regrowth were not included as predictor variables because measurements of their respective rates were not available for the set of biofilter experiments analyzed here. In general, these last two rates would not be useful predictor variables because they are complex (and likely variable) functions of dissolved organic carbon and phosphorus concentrations in urban runoff, and the density and grazing rates of micro- and meso-faunal grazers (e.g., predacious protozoa).<sup>37,53</sup>

Prior to performing the MLR, the variance inflation factor (VIF) was calculated for all predictor variables to identify instances of multicollinearity. No significant multicollinearity was detected ( $\text{VIF} < 5$ ),<sup>54</sup> indicating that all variables were suitable for coevaluation in the MLR analyses. Models were ranked according to the Bayesian Information Criterion (BIC).<sup>55</sup> Candidate best-fit model sets (within 2 BIC units of the highest ranked model) were identified and further evaluated relative to predictive ability using leave-one-out cross validation with Root Mean Squared Error (RMSE) as the validation metric.<sup>56</sup> We then selected the best-fit Total Model and Partial Model as those with the lowest average RMSE (weighted average across all leave-one-out estimates) in their respective candidate sets. The coefficient of determination ( $R^2$ ) was calculated for each best-fit model as an indicator of overall model fit. The relative importance of each predictor variable (i.e., the proportionate contribution made to  $R^2$ ) was estimated using the averaging over ordering method proposed by Lindeman, Merenda, and Gold.<sup>57</sup> Because the relative importance of a predictor can differ from its theoretical importance (i.e., the response magnitude for a given change in the predictor)<sup>57</sup> theoretical importance was assessed using estimated effects plots.

## RESULTS AND DISCUSSION

**Single Collector Contact Efficiencies.** The single collector contact efficiency ( $\eta_0$ ) includes contributions from interception ( $\eta_I$ ), diffusion ( $\eta_D$ ), and gravitational sedimentation ( $\eta_G$ ) (see eq 4 and discussion thereof). To the extent that Tufenkji and Elimelech’s correlation<sup>51</sup> applies to our data set, their theory predicts that Brownian diffusion is the dominant transport

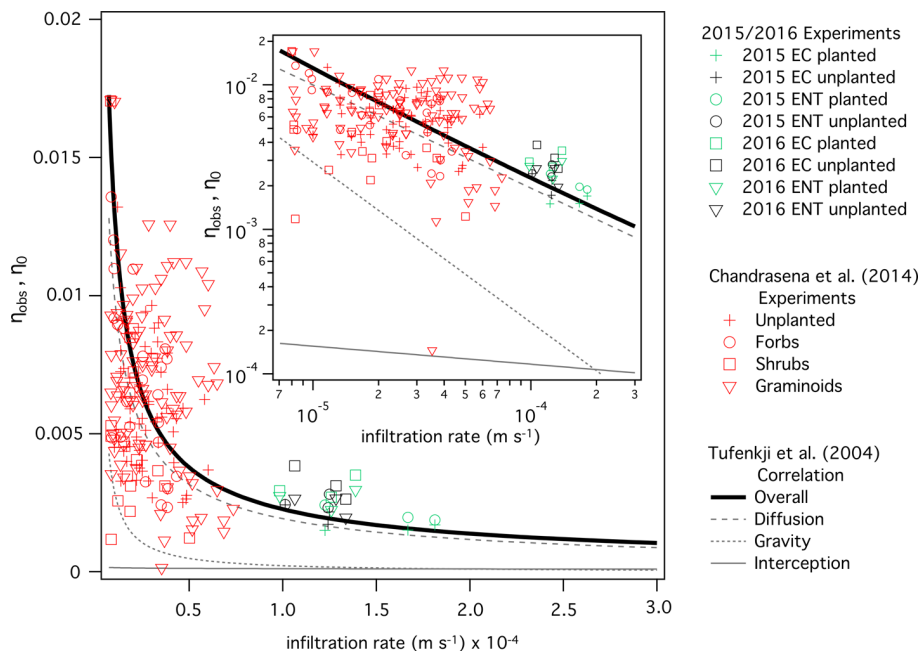


**Figure 1.** Observed single collector contact efficiencies estimated from the 2015/2016 experiments (black and green symbols) and CH's experiments (red symbols), compared to Tufenkji and Elimelech's theoretical correlations for single collector contact efficiency (black (overall) and gray (individual transport mechanisms) curves). Inset: The same comparison, displayed on a log-log plot.

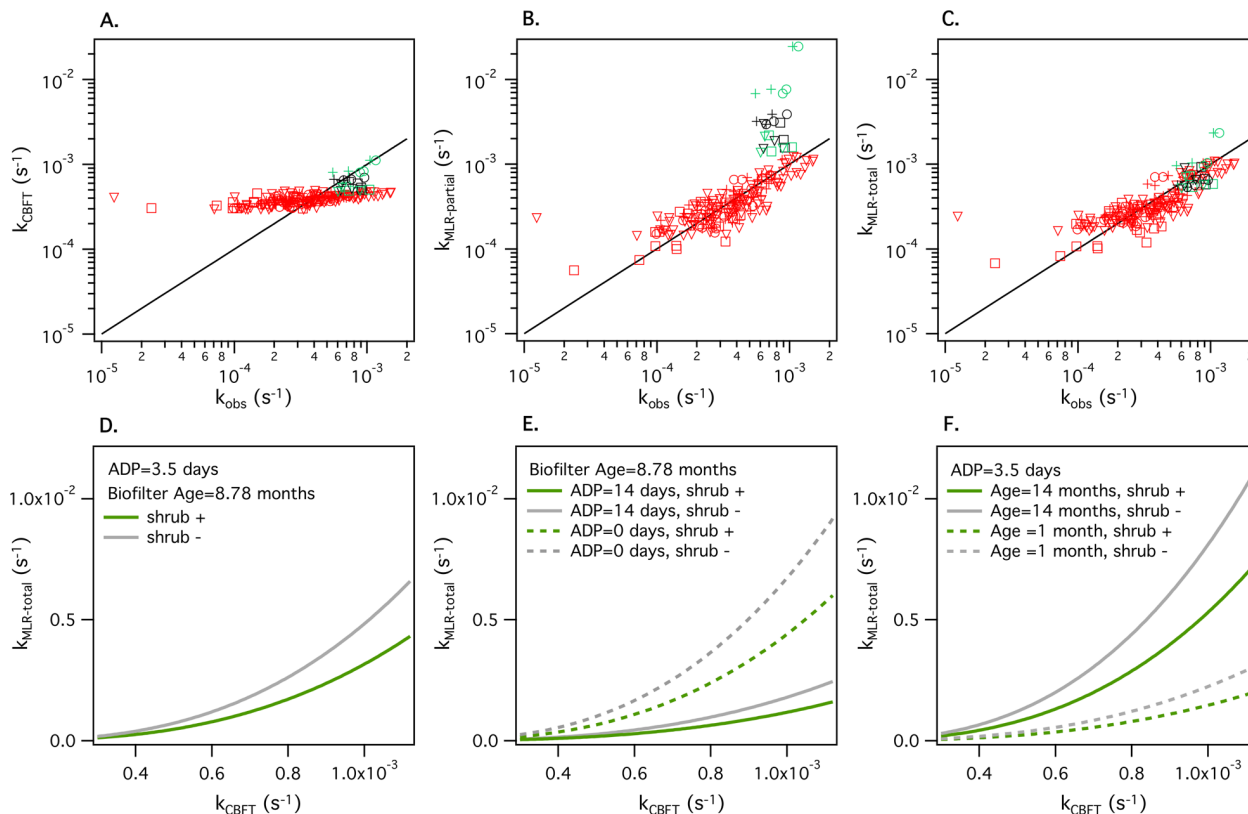


**Figure 2.** (A–C) Cross-plots of experimentally observed first-order FIB removal rate constants and (A) first-order rate constants predicted from CBFT, (B) first-order rate constants predicted from the Partial Model, and (C) first-order rate constants predicted from the Total Model. The black line in each plot is the 1:1 line; symbols are consistent with Figure 1. (D–F) Partial effect plots illustrating how the first-order removal rate constant predicted by the Total Model increases with the CBFT-predicted first-order removal rate constant, and how this response is influenced by shrubs (D–F), antecedent dry period (ADP) (E), and biofilter age (F).

mechanism by which FIB encounter biofilter media; i.e.,  $\eta_0 \approx \eta_D$  over most infiltration rates (compare solid bold and dashed

curves in Figure 1). The theoretical single collector contact efficiency  $\eta_0$  declines sharply with increasing infiltration rate.

This result can be understood by noting that, at higher infiltration rates, FIB are swept past collectors more quickly (thus reducing the opportunity for FIB-grain collisions by one or more transport mechanisms) and hydrodynamic repulsive forces between FIB and grains become stronger on close approach (thus reducing the likelihood that FIB-grain collisions will actually occur). Single collector contact efficiencies calculated from the FIB challenge experiments ( $\eta_{\text{obs}}$ ) follow a similar trend, although there is considerable scatter about the theoretical curve (compare data points with thick solid curve). Interestingly, some of this scatter is plant specific—for example, it appears that biofilters planted with shrubs are consistently biased low relative to Tufenkji and Elimelich's correlation (compare red open squares and dark black curve in Figure 1).

**First-Order Filtration Rates.** CBFT is a poor predictor of the first-order FIB removal rate constants estimated from CH's experiments (red symbols, Figure 2A). In particular, CH's FIB removal rate constants exhibit nearly 100-fold more variability compared to the FIB removal rate constants predicted by CBFT. By contrast, the observed and CBFT-predicted first-order removal rates are in relatively close agreement for the 2015/2016 experiments (black and green symbols, Figure 2A). One interpretation of these results is that CBFT is a better predictor of observed removal rates when the experimental design of the FIB challenge experiments adheres more closely to the assumptions inherent in our analysis of the data—in particular, several of the key assumptions of the dispersed plug flow model (steady flow and fully saturated conditions, see eq 2) were more closely approximated in our 2015/2016 experiment than in CH's experiment. However, the variability in CH's  $k_{\text{obs}}$  may simply reflect the many treatments tested in their study on FIB removal, including five different plant types, two different ADPs, four different biofilter ages, and the presence/absence of submerged zones. Indeed, under realistic field operating conditions it is likely that many different factors—perhaps including CBFT—will influence observed FIB removal rates.

**Multiple Linear Regression.** MLR modeling supports our hypothesis that CBFT can predict observed filtration rates, but only when considered in the context of other environmental, ecological, and biofilter design variables. The selected predictor variables were nearly identical for the Partial Model (CH's data alone) and Total Model (CH's and our 2015/2016 data) (Table S2). The Partial Model consists of four significant predictor variables ( $k_{\text{CBFT}}$ , ADP, column age, and shrub presence/absence) while the Total Model consists of the same four variables plus an additional (fifth) variable “Study”, signaling the presence of a significant study-specific effect (see above discussion of across-study differences). The magnitude of the “Study” effect is evident in Figure 2B,C, where the 2015/2016  $k_{\text{MLR}}$  values (black and green symbols) are clear outliers ( $k_{\text{MLR}} \approx k_{\text{obs}}$ ) when predicted using the best-fit Partial Model (Figure 2B) but fall along the 1:1 line ( $k_{\text{MLR}} \approx k_{\text{obs}}$ ) when “Study” is included in the Total Model (Figure 2C).

Both the Partial Model and Total Model explain a substantial fraction of the observed variance in the FIB removal rate constant  $k_{\text{obs}}$  (approximately 66%; see Table S2). Roughly half of the variance captured by the MLR models is attributable to the CBFT-predicted rate constant  $k_{\text{CBFT}}$  (31% Total Model; 35% Partial Model). The remaining variance, in order of decreasing importance, is attributable to (1) ADP (14% Total Model; 18% Partial Model); (2) Study (8% Total Model; omitted in the Partial Model); (3) column age (7% Total Model; 8% Partial Model); and (4) shrub presence/absence (6% Total Model; 5%

Partial Model, Table S2). These results imply that, while  $k_{\text{CBFT}}$  alone cannot be used to estimate  $k_{\text{obs}}$  (Figure 2A), the former is a strong predictor of the latter when considered together with other (individually subordinate but collectively strong) variables pertaining to hydrology, biofilter maturity, and biofilter ecology (Figure 2B,C). Interestingly, ADP, which appears as the second most important variable in both models (compare averaging over ordering (LMG) scores in Table S2), has been identified as a key factor affecting the removal of stormwater pollutants by biofilters in other studies.<sup>16,17,58–61</sup>

**Partial Effect Plots.** Partial effects plots (calculated from the Total Model) reveal how the influence of CBFT on observed FIB removal rates is modulated by ADP, biofilter age, and the presence of shrubs (Figure 2D–F). Consistent with the results presented in Table S2,  $k_{\text{MLR}}$  increases monotonically with increasing  $k_{\text{CBFT}}$ . However, this relationship is weakened by the presence of shrubs (Figure 2D) and longer ADP (Figure 2E) and is enhanced in older biofilters (Figure 2F). Surprisingly, plants play a relatively minor role in both the Total Model and Partial Model, except to reduce FIB removal rates when the biofilters are planted with shrubs. On its face this result contradicts CH's finding that the choice of plant species strongly influences FIB removal.<sup>39</sup>

This apparent contradiction is resolved by taking into account the distinction between a first-order removal rate for FIB (the focus of this study) and overall FIB removal (the focus of CH's study). We focused on the first-order removal rate because it is the more fundamental parameter; i.e., the overall removal rate achieved by a biofilter will depend on both the rate at which FIB are removed by one or more mechanisms ( $k_{\text{obs}}$ ) and the advective and dispersive transport processes that determine the biofilter's residence time distribution.<sup>47</sup> Thus, plants can affect overall FIB removal in at least three potential ways: (1) creating new mechanisms by which FIB are removed in the biofilter, for example, by growing roots that serve as collectors for FIB,<sup>40</sup> creating habitat for micro- and meso-faunal grazers that remove FIB through predation,<sup>19,37,38,62</sup> and altering the survival rates of FIB through, for example, competition for nutrients;<sup>34</sup> (2) altering the single collector contact efficiency and attachment efficiency through promotion of biofilm growth,<sup>63</sup> generation of surface-active plant exudates,<sup>64</sup> and creation of preferential flow paths that limit stormwater/biofilter media interactions;<sup>65,66</sup> and (3) changing the infiltration rate which, in turn, alters the biofilter's residence time distribution,<sup>66</sup> the single-collector contact efficiency (see Figure 1), and ultimately the first-order filtration rate (see eq 5).

More generally, the above three categories of plant effects can be grouped into those where the plants directly influence FIB removal (categories (1) and (2)) versus those in which plants indirectly influence FIB removal by altering the infiltration rate (category (3)). With the exception of shrubs, our MLR analysis suggests that the type of plants (or even the presence of plants) does not affect the value of  $k_{\text{obs}}$  (see Table S2 and discussion above). Therefore, for the experiments analyzed here, plant selection influences FIB removal indirectly by changing the infiltration rate, not directly by changing the mechanisms of FIB removal, or altering  $\eta_0$  in ways not already accounted for by CBFT theory. This interpretation is consistent with CH's assessment that, relative to FIB removal, “highly performing plant species were associated with lower infiltration rates.”<sup>20</sup>

Our MLR results also suggest that, all else being equal, FIB removal rates increase with increasing biofilter age and decreasing ADP. The influence of increasing biofilter age on

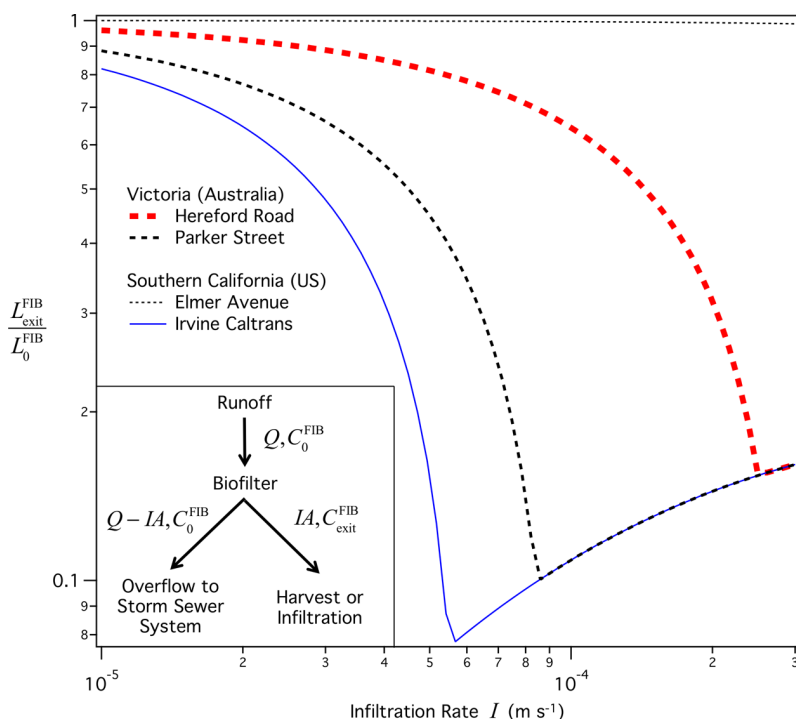


**Figure 3.** Design curves illustrating how the load of FIB exiting a biofilter-catchment system,  $L_{\text{exit}}^{\text{FIB}}/L_0^{\text{FIB}}$ , depends on infiltration rate for four example sites in southern California and the State of Victoria, Australia. Three of the biofilter sites (Irvine Caltrans, Hereford Road, and Parker Street) display an “optimal” infiltration rate, where  $L_{\text{exit}}^{\text{FIB}}/L_0^{\text{FIB}}$  is minimized. Inset: Biofilter water balance, where  $C_0^{\text{FIB}}$  and  $C_{\text{exit}}^{\text{FIB}}$  (MPN  $\text{m}^{-3}$ ) are the concentration of FIB entering and exiting the biofilter, respectively,  $Q$  ( $\text{L s}^{-1}$ ) is the volumetric flow rate of stormwater runoff entering the biofilter,  $I$  ( $\text{m s}^{-1}$ ) is the biofilter infiltration rate, and  $A$  ( $\text{m}^2$ ) is the biofilter surface area. If  $Q > IA$ , then only a fraction ( $IA$ ) of the incoming runoff will be treated by the biofilter while the rest will bypass the biofilter and flow directly to the storm sewer system. Depending on biofilter design, runoff passing through the biofilter can be harvested, infiltrated, or released back to the storm sewer system.

FIB removal rate may reflect an increase in the number of ways FIB are removed by the biofilter as it ages, including “filter ripening” (where previously deposited particles serve as additional collectors in the absence of electrostatic interparticle repulsion),<sup>67</sup> biofilm formation (and associated increases in the attachment efficiency),<sup>63</sup> and/or the progressive growth of micro- and meso-faunal grazers over time.<sup>19,37,38</sup> The influence of ADP on FIB removal rate, however, may reflect the tendency of preferential flow paths (including fissures and macropores) to develop after long ADPs.<sup>34,39</sup> While preferential flow paths are associated with increased infiltration rates (an effect already accounted for by CBFT and hence incorporated into the value of  $k_{\text{CBFT}}$ , see above),<sup>34,39</sup> by “short circuiting” the flow they can also reduce the number of FIB/collector collisions that can occur as FIB quickly pass through the biofilter (an effect not accounted for by CBFT and thus not included in  $k_{\text{CBFT}}$ ). Because ADP can fundamentally alter the mechanisms by which FIB are removed in the biofilter, it is not surprising that this quantity emerges as a secondary but significant predictor of  $k_{\text{obs}}$  in our MLR analysis.

Finally, it is worth noting that different removal mechanisms may operate over different time scales. For example, FIB may attach to media grains by physicochemical filtration over the time scale of a storm, and then undergo permanent removal by micro- or meso-faunal grazing over longer time scales.<sup>19,37</sup>

**Infiltration Rate and Catchment Ratio as Master Design Variables.** The importance of infiltration rate on FIB removal becomes even more evident if one considers not only the biofilter, but also the drainage system within which the biofilter is embedded. As illustrated in Figure 3 (see inset), during a storm event the fraction of runoff from the catchment

( $Q$ ,  $\text{L s}^{-1}$ ) that will be processed by the biofilter is limited by the biofilter’s infiltration rate ( $I$ ,  $\text{m s}^{-1}$ ) and surface area ( $A$ ,  $\text{m}^2$ ). When  $Q < IA$  all runoff will pass through the biofilter, whereas when  $Q > IA$  only a portion of runoff (equal to  $IA$ ) will pass through the biofilter. Thus, at the catchment scale, a potential trade-off arises in which higher infiltration rates increase the volume of runoff passing through the biofilter (all else being equal), but reduce the overall FIB removal achieved for the various reasons described above (e.g., reduction in the single collector contact efficiency and mean residence time in the biofilter).

This potential trade-off can be illustrated by a simple steady-state analysis, in which we assume that minimal on-site storage exists for the runoff (or storage is fully utilized). Under such conditions, the performance of the biofilter/catchment system can be evaluated by quantifying the fraction of FIB load ( $\text{FIB s}^{-1}$ ) flowing out of the catchment ( $L_0^{\text{FIB}}$ ) that is not removed by the biofilter ( $L_{\text{exit}}^{\text{FIB}}$ ):

$$\frac{L_{\text{exit}}^{\text{FIB}}}{L_0^{\text{FIB}}} = \begin{cases} \frac{M_{\text{exit}}^{\text{FIB}}}{M_0^{\text{FIB}}}, & \text{if } \frac{IA}{Q} \geq 1 \\ \frac{IA}{Q} \left( \frac{M_{\text{exit}}^{\text{FIB}}}{M_0^{\text{FIB}}} - 1 \right) + 1, & \text{if } \frac{IA}{Q} < 1 \end{cases}$$

$$\frac{M_{\text{exit}}^{\text{FIB}}}{M_0^{\text{FIB}}} \leq 1 \tag{6}$$

The ratio  $M_{\text{exit}}^{\text{FIB}}/M_0^{\text{FIB}}$  represents the steady-state fraction of FIB mass not removed by the biofilter (see eq 2). We used eq 6 to

estimate  $L_{\text{exit}}^{\text{FIB}}/L_0^{\text{FIB}}$  over a range of biofilter infiltration rates ( $I = 10^{-5}$  to  $3 \times 10^{-4}$  m s<sup>-1</sup>) and for four different biofilter-catchment systems in southern California (Irvine Caltrans and Elmer Avenue) and Melbourne (Hereford Road and Parker Street). For these calculations we assumed: (1) rainfall intensity of  $i = 10$  mm hr<sup>-1</sup>; (2) the biofilters all have the same basic design (i.e., same bed media and depth) but differ in their surface area ( $A$ ) and area of the impervious catchment that drains to the biofilter ( $A_c$ ) (Table S3); and (3) an impervious runoff coefficient of unity (thus all rain falling on the catchment will generate runoff,  $Q = iA_c$ ). The ratio  $M_{\text{exit}}^{\text{FIB}}/M_0^{\text{FIB}}$  appearing in eq 6 was estimated from eq 2 after replacing  $k_{\text{obs}}$  with the Total Model predictions for  $k_{\text{MLR}}$  and assuming: (1) biofilters are one year old; (2) 1 week ADP; (3) shrubs present; and (4) average porosity and dispersivity values obtained from the salt pulse experiments.

For three of the biofilter sites (Irvine Caltrans, Hereford Road, and Parker Street) there is a clear optimal infiltration rate at which FIB mass breakthrough  $L_{\text{exit}}^{\text{FIB}}/L_0^{\text{FIB}}$  is minimized (Figure 3). The FIB removal achieved at this optimal infiltration rate is strongly dependent on the catchment ratio, defined as the ratio of biofilter area to catchment area ( $CR = A/A_c$ , Table S3).<sup>44</sup> The system with the lowest CR (Elmer Avenue) exhibits near complete FIB breakthrough across the full range of infiltration rates evaluated. In this case, the biofilter receives too much runoff (from too large a catchment area) and as a result most of the stormwater generated by the catchment bypasses the biofilter and flows directly to the storm drain (or, in the case of Elmer Avenue, other LID features including porous pavement, bioswales, or an underground infiltration gallery<sup>68</sup>). As CR increases (Hereford < Parker < Caltrans) a larger fraction of the stormwater passes through the biofilter, the optimal infiltration rate shifts toward lower values, and more FIB removal is achieved at the optimal infiltration rate. One of the most pervasive problems with the long-term performance of biofilters is their tendency to accumulate fine particles and clog over time.<sup>69</sup> According to this simple analysis, a decline in infiltration rate (associated with clogging) may increase or decrease FIB removal depending on where a biofilter starts out on the design curves illustrated in Figure 3.

Our MLR model should be viewed as a prototype subject to future refinement, for example to account for the effects of field versus laboratory studies, different classes of microorganisms (viruses, bacteria, protozoans), plant monocultures versus plant polycultures, and soil invertebrates. Practically speaking, the MLR results presented here (plus their future refinements) can be incorporated into standard LID design software packages, such as the U.S. Environmental Protection Agency's Storm Water Management Model (SWMM).<sup>70</sup>

## ■ ASSOCIATED CONTENT

### 📄 Supporting Information

The Supporting Information is available free of charge on the ACS Publications website at DOI: 10.1021/acs.est.7b00752.

Detailed methods for 2015/2016 experiment and salt pulse experiment; calculation of theoretical single collector contact efficiencies; Tables S1, S2, and S3; and additional references (PDF)

## ■ AUTHOR INFORMATION

### Corresponding Author

\*Phone: (949) 824-8277; fax: (949) 824-2541; e-mail: sbgrant@uci.edu (S.B.G.).

## ORCID

Emily A. Parker: 0000-0002-8299-9908

Richard F. Ambrose: 0000-0001-8653-6487

Stanley B. Grant: 0000-0001-6221-7211

## Notes

The authors declare no competing financial interest.

## ■ ACKNOWLEDGMENTS

This work was supported by a grant from the U.S. National Science Foundation Partnerships for International Research and Education (OISE-1243543). The authors thank the following individuals for sampling and logistical support: A. Deletic, D. McCarthy, C. Schang, G. Chandrasena, J. Beam, B. Hatt, R. Williamson, E. Gomez, C. Patel, M. Meyers, S. Chiplunkar, and the 2015 cohort of the Undergraduate PIRE Program (UPP) Down Under. The authors also thank three anonymous reviewers and A. Packman, A. Boehm, A. Afrooz, Morvarid Azizian, Jasper Vrugt, and Jian Peng for their thoughtful suggestions.

## ■ REFERENCES

- Walsh, C. J.; Roy, A. H.; Feminella, J. W.; Cottingham, P. D.; Groffman, P. M.; Morgan, R. P. The urban stream syndrome: current knowledge and the search for a cure. *J. North Am. Benthol. Soc.* **2005**, *24*, 706–723.
- Field, R.; Pitt, R. E.; Fan, C.-Y.; Heaney, J. P.; Stinson, M. K.; DeGuida, R. N.; Perdek, J. M.; Borst, M.; Hsu, K. F.; Urban Wet-Weather. Flows. *Water Environ. Res.* **1997**, *69* (4), 426–444.
- Howarth, R. W.; Sharpley, A.; Walker, D. Sources of nutrient pollution to coastal waters in the United States: Implications for achieving coastal water quality goals. *Estuaries* **2002**, *25* (4), 656–676.
- EPA. *Results of the Nationwide Urban Runoff Program*. Water Planning Division, PB 84–185552; EPA: Washington, DC, 1983.
- Fletcher, T. D.; Deletic, A.; Mitchell, V. G.; Hatt, B. E. Reuse of urban runoff in Australia: A review of recent advances and remaining challenges. *J. Environ. Qual.* **2008**, *37*, 116–127.
- Grant, S. B.; Fletcher, T. D.; Feldman, D.; Saphores, J.-D.; Cook, P. L. M.; Stewardson, M.; Low, K.; Burry, K.; Hamilton, A. J. Adapting urban water systems to a changing climate: Lessons from the Millennium Drought in Southeast Australia. *Environ. Sci. Technol.* **2013**, *47*, 10727–10734.
- Askarizadeh, A.; Rippy, M. A.; Fletcher, T. D.; Feldman, D. L.; Peng, J.; Bowler, P.; Mehring, A. S.; Winfrey, B. K.; Vrugt, J. A.; AghaKouchak, A.; et al. From Rain Tanks to Catchments: Use of Low-Impact Development To Address Hydrologic Symptoms of the Urban Stream Syndrome. *Environ. Sci. Technol.* **2015**, *49* (19), 11264–11280.
- Walsh, C. J.; Fletcher, T. D.; Burns, M. J. Urban stormwater runoff: A new class of environmental flow problem. *PLoS One* **2012**, *7* (9), e45814.
- Grant, S. B.; Saphores, J.-D.; Feldman, D. L.; Hamilton, A. J.; Fletcher, T. D.; Cook, P. L. M.; Stewardson, M.; Sanders, B. F.; Levin, L. A.; Ambrose, R. F.; et al. Taking the “Waste” Out of “Wastewater” for Human Water Security and Ecosystem Sustainability. *Science* **2012**, *337* (6095), 681–686.
- Jiang, S. C.; Lim, K.; Huang, X.; McCarthy, D.; Hamilton, A. J. Human and environmental health risks and benefits associated with use of urban stormwater. *Wiley Interdiscip. Rev.: Water* **2015**, *2*, 683–699.
- Lim, K.; Hamilton, A. J.; Jiang, S. C. Assessment of public health risk associated with viral contamination in harvested urban stormwater for domestic applications. *Sci. Total Environ.* **2015**, *523*, 95–108.
- Payne, E. G. I.; Hatt, B. E.; Deletic, A.; Dobbie, M. F.; McCarthy, D. T.; Chandrasena, G. I. *Adoption Guidelines for Stormwater Biofiltration Systems—Summary Report*; Cooperative Research Centre for Water Sensitive Cities: Melbourne, Australia, 2015.
- Clar, M. L.; Barfield, B. J.; O'Connor, T. P. *Stormwater Best Management Practice Design Guide Vol. 2: Vegetative Biofilters*; EPA/600/



R-04/121A; U.S. Environmental Protection Agency: Washington, DC, 2004.

(14) Wong, T. H. F. Water sensitive urban design—The journey thus far. *Aust. J. Water Resour.* **2006**, *10* (3), 213–222.

(15) Burns, M. J.; Fletcher, T. D.; Walsh, C. J.; Ladson, A. R.; Hatt, B. E. Hydrologic shortcomings of conventional urban stormwater management and opportunities for reform. *Landsc. Urban Plan* **2012**, *105* (3), 230–240.

(16) Chandrasena, G. I.; Pham, T.; Payne, E. G.; Deletic, A.; McCarthy, D. T. *E. coli* removal in laboratory scale stormwater biofilters: Influence of vegetation and submerged zone. *J. Hydrol.* **2014**, *519*, 814–822.

(17) Li, Y. L.; Deletic, A.; Alcazar, L.; Bratieres, K.; Fletcher, T. D.; McCarthy, D. Removal of *Clostridium perfringens*, *Escherichia coli* and F-RNA coliphages by stormwater biofilters. *Ecol. Eng.* **2012**, *49*, 137–145.

(18) Mohanty, S. K.; Torkelson, A. A.; Dodd, H.; Nelson, K. L.; Boehm, A. B. Engineering Solutions to Improve the Removal of Fecal Indicator Bacteria by Bioinfiltration Systems during Intermittent Flow of Stormwater. *Environ. Sci. Technol.* **2013**, *47* (19), 10791–10798.

(19) Zhang, L.; Seagren, E.; Davis, A.; Karns, J. Long-Term Sustainability of *Escherichia Coli* Removal in Conventional Bioretention Media. *J. Environ. Eng.* **2011**, *137* (8), 669–677.

(20) Chandrasena, G. I.; Deletic, A.; Ellerton, J.; McCarthy, D. T. Evaluating *Escherichia coli* removal performance in stormwater biofilters: a laboratory-scale study. *Water Sci. Technol.* **2012**, *66*, 1132–1138.

(21) Mohanty, S. K.; Boehm, A. B. *Escherichia coli* Removal in Biochar-Augmented Biofilter: Effect of Infiltration Rate, Initial Bacterial Concentration, Biochar Particle Size, and Presence of Compost. *Environ. Sci. Technol.* **2014**, *48* (19), 11535–11542.

(22) Hathaway, J. M.; Hunt, W. F.; Graves, A. K.; Wright, J. D. Field Evaluation of Bioretention Indicator Bacteria Sequestration in Wilmington, North Carolina. *J. Environ. Eng.* **2011**, *137* (12), 1103–1113.

(23) Prüss, A. Review of epidemiological studies on health effects from exposure to recreational water. *Int. J. Epidemiol.* **1998**, *27* (1), 1–9.

(24) Haile, R. W.; Witte, J. S.; Gold, M.; Cressey, R.; McGee, C.; Millikan, R. C.; Glasser, A.; Harawa, N.; Ervin, C.; Harmon, P.; et al. The health effects of swimming in ocean water contaminated by storm drain runoff. *Epidemiol. Camb. Mass* **1999**, *10* (4), 355–363.

(25) Sidhu, J. P. S.; Ahmed, W.; Gernjak, W.; Aryal, R.; McCarthy, D.; Palmer, A.; Kolotelo, P.; Toze, S. Sewage pollution in urban stormwater runoff as evident from the widespread presence of multiple microbial and chemical source tracking markers. *Sci. Total Environ.* **2013**, *463–464*, 488–496.

(26) Grebel, J. E.; Mohanty, S. K.; Torkelson, A. A.; Boehm, A. B.; Higgins, C. P.; Maxwell, R. M.; Nelson, K. L.; Sedlak, D. L. Engineered Infiltration Systems for Urban Stormwater Reclamation. *Environ. Eng. Sci.* **2013**, *30* (8), 437–454.

(27) Ahn, J. H.; Grant, S. B.; Surbeck, C. Q.; Digiaco, P. M.; Nezhin, N. P.; Jiang, S. C. Coastal water quality impact of stormwater runoff from an urban watershed in Southern California. *Environ. Sci. Technol.* **2005**, *39* (16), 5940–5953.

(28) Reeves, R. L.; Grant, S. B.; Mrse, R. D.; Oancea, C. M. C.; Sanders, B. F.; Boehm, A. B. Scaling and management of fecal indicator bacteria in runoff from a coastal urban watershed in Southern California. *Environ. Sci. Technol.* **2004**, *38* (9), 2637–2648.

(29) EPA. *Total Maximum Daily Loads with Stormwater Sources: A Summary of 17 TMDLs*, EPA 841-R-07-002. EPA: Washington, DC, 2007.

(30) Given, S.; Pendleton, L. H.; Boehm, A. B. Regional public health cost estimates of contaminated coastal waters: A case study of gastroenteritis at Southern California Beaches. *Environ. Sci. Technol.* **2006**, *40* (16), 4851–4858.

(31) Pendleton, L. The economics of using ocean observing systems to improve beach closure policy. *Coastal Management* **2008**, *36* (2), 165–178.

(32) Point Loma Nazarene University: *Meeting Water Quality Standards for San Diego's Recreational Waters: A Cost Benefit Analysis*; Fermanian Business and Economic Institute: San Diego, CA, 2013.

(33) Davis, A. P.; Hunt, W. F.; Traver, R. G.; Clar, M. Bioretention technology: Overview of current practice and future needs. *J. Environ. Eng.* **2009**, *135* (3), 109–117.

(34) Rippy, M. A. Meeting the criteria: linking biofilter design to fecal indicator bacteria removal. *Wiley Interdiscip. Rev.: Water* **2015**, *2*, 577–592.

(35) Yao, K.-M.; Habibian, M. T.; O'Melia, C. R. Water and waste water filtration: Concepts and applications. *Environ. Sci. Technol.* **1971**, *5* (11), 1105–1112.

(36) Logan, B. E.; Jewett, D. G.; Arnold, R. G.; Bouwer, E. J.; O'Melia, C. R. Clarification of Clean-Bed Filtration Models. *J. Environ. Eng.* **1995**, *121* (12), 869–873.

(37) Zhang, L.; Seagren, E. A.; Davis, A. P.; Karns, J. S. The Capture and Destruction of *Escherichia coli* from Simulated Urban Runoff Using Conventional Bioretention Media and Iron Oxide-coated Sand. *Water Environ. Res.* **2010**, *82*, 701–714.

(38) Peng, J.; Cao, Y.; Rippy, M. A.; Afroz, A. R. M. N.; Grant, S. B. Indicator and Pathogen Removal by Low Impact Development Best Management Practices. *Water* **2016**, *8* (12), 600.

(39) Chandrasena, G. I.; Deletic, A.; McCarthy, D. T. Evaluating *Escherichia coli* removal performance in stormwater biofilters: a preliminary modeling approach. *Water Sci. Technol.* **2013**, *67*, 2467–2475.

(40) Khatiwada, N. R.; Polprasert, C. Kinetics of Fecal Coliform Removal in Constructed Wetlands. *Water Sci. Technol.* **1999**, *40* (3), 109–116.

(41) Bradford, S. A.; Bettahar, M.; Simunek, J.; van Genuchten, M. T. Straining and Attachment of Colloids in Physically Heterogeneous Porous Media. *Vadose Zone J.* **2004**, *3*, 384–394.

(42) Tufenkji, N. Modeling microbial transport in porous media: Traditional approaches and recent developments. *Adv. Water Resour.* **2007**, *30*, 1455–1469.

(43) Duncan, H. P. *Urban Stormwater Quality: A Statistical Overview*. Cooperative Research Centre for Catchment Hydrology: Melbourne, Australia, 1999.

(44) Ambrose, R. F.; Winfrey, B. K. Comparison of stormwater biofiltration systems in Southeast Australia and Southern California. *Wiley Interdiscip. Rev.: Water* **2015**, *2*, 131–146.

(45) *Facility for Advancing Water Biofiltration (FAWB). Adoption Guidelines for Stormwater Bioinfiltration Systems*; Monash University: Melbourne, Australia, 2009, pp 1–38.

(46) Han, Y.; Lau, S.; Kayhanian, M.; Stenstrom, M. K. Characteristics of Highway Stormwater Runoff. *Water Environ. Res.* **2006**, *78* (12), 2377–2388.

(47) Levenspiel, O. *Chemical Reaction Engineering*; Wiley: New York, 1972.

(48) Vrugt, J. A.; ter Braak, C. G. F.; Diks, C. G. H.; Higdón, D.; Robinson, B. A.; Hyman, J. M. Accelerating Markov chain Monte Carlo simulation by differential evolution with self-adaptive randomized subspace sampling. *Int. J. Nonlinear Sci. Numer. Simul.* **2009**, *10*, 273–290.

(49) Vrugt, J. A. Markov chain Monte Carlo simulation using the DREAM software package: Theory, concepts, and MATLAB implementation. *Environ. Model. Softw.* **2016**, *75*, 273–316.

(50) Wehner, J. F.; Wilhelm, R. H. Boundary conditions of flow reactor. *Chem. Eng. Sci.* **1956**, *6*, 89–93.

(51) Tufenkji, N.; Elimelech, M. Correlation Equation for Predicting Single-Collector Efficiency in Physicochemical Filtration in Saturated Porous Media. *Environ. Sci. Technol.* **2004**, *38* (2), 529–536.

(52) R Core Team. *R: A Language and Environment for Statistical Computing*; R Foundation for Statistical Computing: Vienna, Austria, 2013, URL: <http://www.R-project.org/>.

(53) Surbeck, C. Q.; Jiang, S. C.; Grant, S. B. Ecological control of fecal indicator bacteria in an urban stream. *Environ. Sci. Technol.* **2010**, *44* (2), 631–637.

(54) Zuur, A. F.; Ieno, E. N.; Elphick, C. S. A protocol for data exploration to avoid common statistical problems. *Method. Ecol. Evol.* **2010**, *1*, 3–14.

- (55) Schwarz, G. Estimating the dimension of a model. *Ann. Statist.* **1978**, *6*, 461–464.
- (56) Hawkins, D. M.; Basak, S. C.; Mills, D. Assessing model fit by cross-validation. *J. Chem. Inf. Comput. Sci.* **2003**, *43*, 579–586.
- (57) Gromping, U. Relative Importance for Linear Regression in R: The Package relaimpo. *J. Stat. Softw.* **2006**, *17* (1), 1–27.
- (58) Blecken, G.-T.; Zinger, Y.; Deletic, A.; Fletcher, T. D.; Viklander, M. Influence of intermittent wetting and drying conditions on heavy metal removal by stormwater biofilters. *Water Res.* **2009**, *43*, 4590–4598.
- (59) Payne, E. G. I.; Pham, T.; Cook, P. L. M.; Fletcher, T. D.; Hatt, B. E.; Deletic, A. Biofilter design for effective nitrogen removal from stormwater – influence of plant species, inflow hydrology and use of a saturated zone. *Water Sci. Technol.* **2014**, *69* (6), 1312–1319.
- (60) Read, J.; Wevill, T.; Fletcher, T. D.; Deletic, A. Variation among plant species in pollutant removal from stormwater in biofiltration systems. *Water Res.* **2008**, *42*, 893–902.
- (61) Read, J.; Fletcher, T. D.; Wevill, T.; Deletic, A. Plant traits that enhance pollutant removal from stormwater in biofiltration systems. *Int. J. Phytorem.* **2009**, *12*, 34–53.
- (62) Bonkowski, M.; Villenave, C.; Griffiths, B. Rhizosphere fauna: the functional and structural diversity of intimate interactions of soil fauna with plant roots. *Plant Soil* **2009**, *321* (1), 213–233.
- (63) Afroz, A. R. M.; Boehm, A. B. *Escherichia coli* removal in biochar-modified biofilters: effects of biofilm. *PLoS One* **2016**, *11* (12), e0167489.
- (64) Foppen, J. W.; Liem, Y.; Schijven, J. Effect of humic acid on the attachment of *Escherichia coli* in columns of goethite-coated sand. *Water Res.* **2008**, *42*, 211–219.
- (65) Archer, N. A. L.; Quinton, J. N.; Hess, T. M. Below-ground relationships of soil texture, roots and hydraulic conductivity in two-phase mosaic vegetation in South-east Spain. *J. Arid. Environ.* **2002**, *52*, 535–553.
- (66) Virahsawmy, H. K.; Stewardson, M. J.; Vietz, G.; Fletcher, T. D. Factors that affect the hydraulic performance of raingardens: implications for design and maintenance. *Water Sci. Technol.* **2014**, *69* (5), 982–988.
- (67) O'Melia, C. R.; Ali, W. The role of retained particles in deep bed filtration. *Progr. Water Technol.* **1979**, *10*, 167–182.
- (68) Belden, E.; Antos, M.; Morris, K.; Steele, N. L.C. Sustainable Infrastructure: The Elmer Avenue Neighborhood Retrofit. *Urban Coast* **2012**, *3* (1), 92–100.
- (69) Kandra, H.; McCarthy, D.; Deletic, A. Assessment of the Impact of Stormwater Characteristics on Clogging in Stormwater Filters. *Water Resour. Manage.* **2015**, *29* (4), 1031–1048.
- (70) EPA, 2015. *Storm Water Management Model User's Manual Version 5.1*, EPA 600/%-14/413b; EPA: Washington, DC.